THE JOURNAL OF PHYSICAL CHEMISTRY A

Article

pubs.acs.org/JPCA

Production of H and O(^{3}P) Atoms in the Reaction of CH_2 with O_2

Pei-Fang Lee, Hiroyuki Matsui,* Wei-Yu Chen, and Niann-Shiah Wang*

Department of Applied Chemistry, National Chiao Tung University, 1001, Ta Hsueh Road, Hsinchu 30010, Taiwan

ABSTRACT: The reaction $CH_2 + O_2 \rightarrow$ products has been studied by using atomic resonance absorption spectrometry (ARAS) of H and O(^{3}P) atoms behind reflected shock waves over 1850−2050 K and 2.1−1.7 atm. Measurements of [H] and [O] are conducted using mixtures of highly diluted CH_2I_2 (0.2 and 0.4 ppm) with excess O_2 (100 and 262 ppm) in Ar; comparative measurement of [H] in the 0.2 and 0.4 ppm CH_2I_2 + 300 ppm H_2 mixture has been conducted simultaneously to confirm the initial concentration of CH_2. The apparent reaction rate of $CH_2 + O_2$ (k_2'), including the contributions of $^3CH_2 + O_2 \rightarrow$ products (2) and $^1CH_2 + O_2 \rightarrow$ products (3), has been measured from the evolutions of [H] and [O] and summarized as k_2'/cm^3 molecule^{-1} s^{-1} = (1.90 ± 0.31) × 10^{-11}. The contribution of $^1CH_2 + O_2$ reaction on the measured k_2' has been evaluated as 0.15 ± 0.04, with an assumption that k_3 is independent of temperature and given by the result measured at room temperature [Langford, A. O.; Petek, H.; Moore, C. B. *J. Chem. Phys.* **1983**, 78, 6650−6659]. The net rate for the $^3CH_2 + O_2$ reaction is given as k_2/cm^3 molecule^{-1} s^{-1} = (1.69 ± 0.31) × 10^{-11}. The result on k_2 in this study is found to be consistent with the extrapolation of the previous work at lower temperature range of 295−600 K. [Vinckler, C.; Debruyn, W. *J. Phys. Chem.* **1979**, 83, 2057−2062]; these results can be summarized as k_2/cm^3 molecule^{-1} s^{-1} = 2.74 × 10^{-11} exp(−874/T), (T = 295−2050 K). The apparent production yields of H and O atoms for the reaction channels $^{1,3}CH_2 + O_2 \rightarrow$ H + products (2a, 3a) and $^{1,3}CH_2 + O_2 \rightarrow$ O(^{3}P) + products (2b, 3b) have been evaluated as $\phi_{2a}' = 0.59 \pm 0.06$ and $\phi_{2b}' = 0.23 \pm 0.06$, respectively. The contributions of $^1CH_2 + O_2$ reaction on measured ϕ_{2a}' and ϕ_{2b}' are indicated to be minor; the net branching fractions for the $^3CH_2+O_2$ reaction are estimated as $\phi_{2a} = 0.58 \pm 0.06$ and $\phi_{2b} = 0.25 \pm 0.06$. No obvious temperature dependence is indicated in the measured rate constant nor in the branching fractions of H and O atoms. The mechanism of the reaction of CH_2 with O_2 is discussed based on the result of the present study together with those of the previous theoretical/experimental studies.

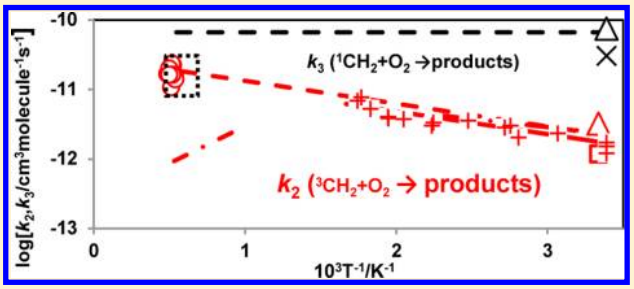

1. INTRODUCTION

Investigation of the reaction of CH_2 ($\tilde{X}^3B_1$) and CH_2 ($\tilde{a}^1A_1$) (denoted as $^3CH_2$ and $^1CH_2$, respectively) with O_2 is still a challenging subject, in spite of extensive theoretical and experimental explorations over the last several decades.

The reaction is too complicated (associated with multiple potential energy surfaces leading to many possible product channels) to get a clear insight into the detailed reaction mechanism.[1−13] The reaction intermediate CH_2O_2 (starting from $^3CH_2 + O_2$) is called a Criegee intermediate,[2] and is regarded as a key species in the ozonolysis of alkenes in atmospheric reaction cycle.[14−16] This reaction is also important in the combustion of hydrocarbon fuels.[17−19]

The rate of the $CH_2 + O_2$ reaction has been measured by several groups.[20−25] Vinckler and Debruyn conducted a mass-spectrometric measurement of the rate for the $^3CH_2 + O_2$ reaction over 295−600 K:[21] their result agrees well with those by detection of $^3CH_2$ by LMR spectrometers[24] and the infrared diode laser probe method[22] at around room temperature. Only one data has been reported at high temperature range (T > 1000 K) by using a shock tube technique combined with the atomic resonance absorption spectrometry (ARAS) technique,[23,25] but the extrapolation of the result of Vinckler and Debruyn with the experimentally observed activation energy of 1500 cal/mol to the high temperature range is inconsistent with the result of the shock tube measurement.

For the reaction of $^1CH_2 + O_2$, Ashford et al. reported the rate of removal (reaction + collisional quenching) at 298 K as 3 × 10^{-11} cm^3 molecule^{-1} s^{-1} via the laser induced fluorescence (LIF) detection method.[26] Langford et al. also studied the removal rate of $^1CH_2$ in the $^1CH_2 + O_2$ reaction as 7.4 × 10^{-11} cm^3 molecule^{-1} s^{-1} at 295 K by using resonance absorption of $^1CH_2$ with a continuous wave (cw) laser at 590−610 nm.[27] On the basis of the latter result, GRI mech-3.0 employs the net rate of 6.64 × 10^{-11} cm^3 molecule^{-1} s^{-1} (independent of temperature) in the reaction model for the combustion of natural gas.[18]

Much less information is available for the detailed reaction mechanism and product branching of the title reaction. It is generally accepted that the first step of the $^3CH_2 + O_2$ reaction is to form a CH_2OO radical (Criegee), then rearrangement to dioxirane, dioxymethane, and highly excited formic acid may take place prior to the formation of the final products: i.e.,

Received: July 18, 2012
Revised: August 20, 2012
Published: August 20, 2012

dx.doi.org/10.1021/jp307140z | *J. Phys. Chem. A* 2012, 116, 9245−9254

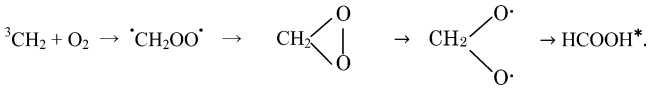

In this study, evolutions of H and O atoms produced in the shock heated samples of 0.2−0.4 ppm CH_2I_2 with 100−263 ppm O_2 diluted in Ar have been quantitatively measured between 1850 and 2050 K, where CH_2I_2 has been used to supply $^3CH_2$ by utilizing sequential C−I bond fission, i.e.,

$$CH_2I_2 + M \rightarrow CH_2I + I + M \quad (1a)$$

and

$$CH_2I + M \rightarrow {}^3CH_2 + I + M \quad (1b)$$

Thermal decomposition of CH_2I_2 has been studied by monitoring evolutions of I atoms using a low concentration of CH_2I_2 (0.1 ppm CH_2I_2 in Ar) in our previous study.[28] CH_2I_2 is suggested to be a clean source to supply $^3CH_2$ below 2000 K, since sequential C−I bond fission processes are confirmed to be dominant over other product channels, and the rate for producing $^3CH_2$ is found to be $\ln(k_2/\ \mathrm{cm^3\ molecule^{-1}\ s^{-1}}) = -(17.28 \pm 0.79) - (30.17 \pm 1.40) \times 10^3/T$, which is sufficiently fast to study the title reaction at $T > 1800$ K.

The reaction $CH_2I + O_2$ has been studied recently; the rate is given by $k(CH_2I + O_2) = (1.39 \pm 0.01) \times 10^{-12}\ (T/300\ \mathrm{K})^{-1.55\pm0.06}\ \mathrm{cm^3\ molecule^{-1}\ s^{-1}}$ for $T = 222$−450 K,[29] and the main product channel has been assigned as CH_2O_2+I.[30]

The contribution of the reaction of the intermediate CH_2I with O_2 is negligibly small for the experimental conditions of this study at an elevated temperature range, then the reactions to be considered in the study of the low concentration CH_2I_2 + excess O_2 in Ar can be simplified as

$$CH_2I_2 + Ar \rightarrow {}^3CH_2 + 2I + Ar \quad (1)$$

$$^3CH_2 + O_2 \rightarrow \text{products} \quad (2)$$

$$^1CH_2 + O_2 \rightarrow \text{products} \quad (3)$$

$$^1CH_2 + Ar \leftrightarrow {}^3CH_2 + Ar \quad (4)$$

$$H + O_2 \rightarrow OH + O \quad (5)$$

For the convenience of analyzing the experimental data on the evolutions of H and O atoms, the product channels of reactions 2 and 3 may be expressed as follows:

$$^3CH_2 + O_2 \rightarrow H + \text{products} \quad (2a)$$

$$^3CH_2 + O_2 \rightarrow O + \text{products} \quad (2b)$$

$$^3CH_2 + O_2 \rightarrow \text{products without H and O} \quad (2c)$$

and

$$^1CH_2 + O_2 \rightarrow H + \text{products} \quad (3a)$$

$$^1CH_2 + O_2 \rightarrow O + \text{products} \quad (3b)$$

$$^1CH_2 + O_2 \rightarrow \text{products without H and O} \quad (3c)$$

Here, the reaction channel associated with the simultaneous production of H and O atoms is not taken into consideration, i.e., the branching fractions for reactions 2c and 3c are given by $\phi_{2c} = 1 - (\phi_{2a} + \phi_{2b})$ and $\phi_{3c} = 1 - (\phi_{3a} + \phi_{3b})$, where $\phi_{2a} = k_{2a}/k_2$, $\phi_{2b} = k_{2b}/k_2$, $\phi_{3a} = k_{3a}/k_3$, and $\phi_{3b} = k_{3b}/k_3$.

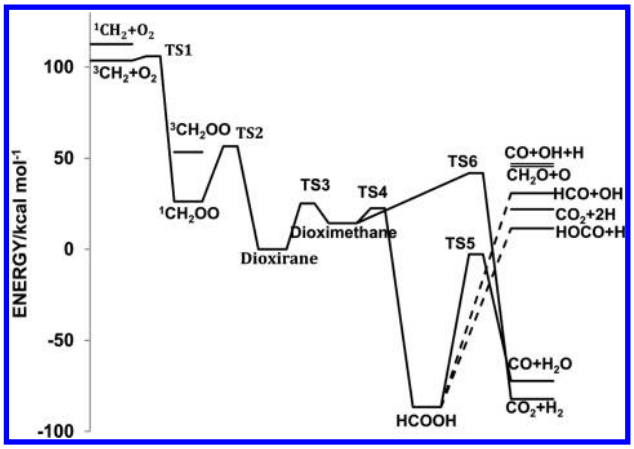

Figure 1. Schematic of the potential energy diagram of the $CH_2 + O_2$ reaction system. Relative energy compared with dioxirane is demonstrated; energies for the reaction intermediates and the transition states TS1-TS6 are taken from ref 13, and speculated reaction paths are illustrated by dotted lines.

A schematic energy diagram for this reaction system is shown in Figure 1; there seems to be many product channels energetically allowed. In order to discuss the yields of H and O atoms, it may be convenient to label the possible product channels as follows:

$$^3CH_2 + O_2 \rightarrow HCO + OH \quad (2a\text{-}1)$$

$$\rightarrow H + CO + OH \quad (2a\text{-}2)$$

$$\rightarrow HOCO + H \quad (2a\text{-}3)$$

$$\rightarrow 2H + CO_2 \quad (2a\text{-}4)$$

$$\rightarrow CH_2O + O(^3P) \quad (2b\text{-}1)$$

$$\rightarrow CO_2 + H_2 \quad (2c\text{-}1)$$

$$\rightarrow CO + H_2O \quad (2c\text{-}2)$$

$$\rightarrow \text{other products (without H and O)} \quad (2c\text{-}3)$$

The reactions 2a-1 to 2a-4 correspond to the formation of H atoms (reaction 2a), since HCO and HOCO should rapidly decompose at high temperature to form H + CO and H + CO_2, respectively. By contrast, only a single reaction channel (2b-1) may be a candidate for the formation of O atoms (2b).

Also, due to the very rapid collisional excitation of $^3CH_2$ to $^1CH_2$ (−4), it is necessary to consider the same reaction scheme as above for the reaction $^1CH_2 + O_2$ (3) for the study at high temperature, i.e.,

$$^1CH_2 + O_2 \rightarrow HCO + OH \quad (3a\text{-}1)$$

$$\rightarrow H + CO + OH \quad (3a\text{-}2)$$

$$\rightarrow HOCO + H \quad (3a\text{-}3)$$

$$\rightarrow 2H + CO_2 \quad (3a\text{-}4)$$

$$\rightarrow CH_2O + O(^3P) \quad (3b\text{-}1)$$

$$\rightarrow CO_2 + H_2 \quad (3c\text{-}1)$$

$$\rightarrow CO + H_2O \quad (3c\text{-}2)$$

$$\rightarrow \text{other products (without H and O)} \quad (3c\text{-}3)$$

dx.doi.org/10.1021/jp307140z | J. Phys. Chem. A 2012, 116, 9245−9254

Table 1. Summary of the Experimental Conditions for the Study on the Reaction $CH_2 + O_2$ and the Evaluated Rates and Branching Fractions[a]

T/K	P/atm	$[CH_2I_2]_0$[b]	$[O_2]$[c]	[Ar][d]	K_{c4}	k_2'[e]	k_2[e]	ϕ_{2a}'[f]	ϕ_{2a}[g]	ϕ_{2b}'[f]	ϕ_{2b}[h]
Measurement of [H]											
0.4 ppm CH_2I_2 + 100 ppm O_2											
1858	2.1	3.13	0.83	8.28	0.041	1.76 ± 0.36	1.49 ± 0.34	0.60 ± 0.030	0.58		
1954	1.98	2.98	0.74	7.44	0.046	1.33 ± 0.40	1.02 ± 0.38	0.60 ± 0.031	0.57		
2055	1.77	2.52	0.63	6.31	0.051	1.91 ± 0.48	1.57 ± 0.46	0.61 ± 0.04	0.59		
0.2 ppm CH_2I_2 + 100 ppm O_2											
1858	2.09	1.65	0.82	8.24	0.041	1.65 ± 0.36	1.38 ± 0.34	0.69 ± 0.029	0.69		
1905	2.04	1.57	0.79	7.87	0.043	1.79 ± 0.38	1.50 ± 0.65	0.60 ± 0.030	0.58		
1938	2.01	1.52	0.76	7.62	0.045	1.87 ± 0.49	1.57 ± 0.46	0.62 ± 0.031	0.6		
2005	1.91	1.4	0.7	7.01	0.049	1.94 ± 0.43	1.62 ± 0.41	0.69 ± 0.030	0.58		
Measurement of [O]											
0.4 ppm CH_2I_2 + 100 ppm O_2											
1895	2.04	3.14	0.78	7.84	0.043	1.84 ± 0.38	1.56 ± 0.36	0.51 ± 0.04	0.48	0.21 ± 0.04	0.25
1935	2.01	3.05	0.76	7.61	0.045	2.16 ± 0.40	1.86 ± 0.37	0.63 ± 0.04	0.62	0.26 ± 0.04	0.30
1994	1.9	2.79	0.7	6.99	0.048	2.08 ± 0.41	1.76 ± 0.38	0.58 ± 0.03	0.56	0.22 ± 0.04	0.26
0.2 ppm CH_2I_2 + 100 ppm O_2											
1858	2.09	1.65	0.82	8.24	0.041	1.73 ± 0.30	1.46 ± 0.28	0.48 ± 0.05	0.44	0.25 ± 0.04	0.30
1905	2.04	1.57	0.79	7.87	0.043	2.42 ± 0.33	2.13 ± 0.30	0.54 ± 0.04	0.52	0.24 ± 0.03	0.27
1937	2.01	1.52	0.76	7.61	0.045	2.54 ± 0.39	2.24 ± 0.36	0.60 ± 0.03	0.59	0.25 ± 0.03	0.28
2002	1.91	1.4	0.7	7.01	0.049	2.21 ± 0.43	1.89 ± 0.40	0.53 ± 0.05	0.51	0.25 ± 0.05	0.29
0.4 ppm CH_2I_2 + 262 ppm O_2											
1850	2.01	3.19	2.15	8.22	0.04	1.41 ± 0.18	1.34 ± 0.16	0.62 ± 0.04	0.61	0.21 ± 0.02	0.25
1921	1.99	3.04	1.99	7.59	0.044	1.84 ± 0.24	1.55 ± 0.21	0.62 ± 0.05	0.61	0.20 ± 0.03	0.24
2005	1.91	2.79	1.83	6.98	0.049	1.86 ± 0.31	1.54 ± 0.29	0.58 ± 0.04	0.55	0.21 ± 0.05	0.25

[a]All the measurements for H and O atoms have been repeated two times at the same shock wave condition so as to confirm the reproducibility. Experimental conditions summarized in this table are shown by the averaged values. Uncertainties of temperature brought by the fluctuation of the incident shock wave velocity are within ±5 K. [b]10^{12} molecules cm^{-3}. [c]10^{15} molecules cm^{-3}. [d]10^{18} molecules cm^{-3}. [e]10^{-11} cm^3 molecule^{-1} s^{-1}. [f]$\phi_{2a}' = \phi_{2a}$, if $\phi_{3a} = \phi_{2a}$; also $\phi_{2b}' = \phi_{2b}$, if $\phi_{3b} = \phi_{2b}$ (see text). [g]It is assumed that $\phi_{3a} = 0.7$.[18] [h]It is assumed that $\phi_{3b} = 0$.[18]

Experimental examination of the product branching for the reaction $^3CH_2 + O_2$ was conducted by the IR diode laser absorption method at room temperature for the stable products CO_2, CO, and CH_2O:[31] the branching fractions for the production channels of CO_2, CO, and CH_2O were indicated as 0.40 ± (0.07−0.09), 0.34 ± 0.02, and 0.16 ± 0.04, respectively. Also OH production was suggested to be about the same amount of CO (or HCO) from the analysis of kinetic simulation. Measurement of the product branching for H and O atoms (assigned in the present study as ϕ_{2a} and ϕ_{2b}, respectively) was conducted by a shock-tube/ARAS technique[23,25] at elevated temperature T = 1000−1700 K, and the result was indicated to be $\phi_{2a} \cong 0.2$ and $\phi_{2b} \cong 0.1$.

The issue of the present study is to reinvestigate the mechanism of the reaction, $CH_2 + O_2 \rightarrow$ products, by using a shock tube/ARAS system for H and O(^{3}P) atoms; the main difference of our study from the previous one[23,25] is to employ much lower concentrations of the source for $^3CH_2$ (0.2−0.4 ppm, less than 1/100 of the previous study) to reduce the contributions of the secondary reactions.

2. EXPERIMENTAL SYSTEM

A diaphragmless shock tube apparatus (length 5.9 m and i.d. 7.6 cm) with an ARAS detection system was used. The details of the experiments were described in previous studies.[32,33] For the measurements of temporal profiles of [H] and [O], resonant atomic absorption of H atoms at 121.6 nm and that of O atoms at 130.5 nm was monitored by using a microwave-discharge lamp filtered with a VUV monochromator with f = 20 cm, and detected by a solar-blind photomultiplier tube. Gas mixture of 1% H_2 or O_2 diluted in a He flow of 10 Torr was supplied in the microwave-discharge lamp. VUV light passed perpendicularly through the MgF_2 windows at 4 cm upstream of the end plate of the shock tube. All the measurements were conducted behind reflected shock waves, and the experimental temperature and the concentrations were evaluated by using the ideal one-dimensional Rankine−Hugoniot relations.

Decomposition of C_2H_5I was used to construct a calibration curve of the concentration of H atoms as reported in our previous papers,[28,32] where, the branching fraction for the reaction channel $C_2H_5I + Ar \rightarrow C_2H_5 + I + Ar$ was given as 0.90 ± 0.05. A calibration curve for O(^{3}P) atoms was constructed using reactions $H + O_2 \rightarrow OH + O(^3P)$ and thermal decomposition $N_2O + Ar \rightarrow N_2 + O(^3P) + Ar$ in the mixtures of 0.3−0.5 ppm C_2H_5I + 300 ppm O_2 (T = 1800−2000 K), and 0.1−0.3 ppm N_2O (T = 2800−3300 K) diluted in Ar, respectively. Temperature dependence on the calibration curve of O atoms was not detected, i.e., the relationship of [O] against absorbance is consistent each other for these different precursors in the different temperature ranges. The sensitivity for H and O atoms in the present experimental system is high; a detection limit of (1−2) × 10^{11} atom/cm^3 is attained. The signal-to-noise (S/N) ratio for the observed signal intensity for O atoms is about 1/3 of that for H atoms. The response time of the present detection system is about 25 μs (determined from the profiles of H and I atoms produced in the C_2H_5I decomposition); it is necessary to choose suitable experimental conditions adequate to analyze the evolutions of

dx.doi.org/10.1021/jp307140z | J. Phys. Chem. A 2012, 116, 9245−9254

H and O to evaluate the rates and branching fractions with sufficient reliability.

As a standard routine of this study, evacuation of the sample cylinders and the test section of the shock tube has been continued with baking process under a high vacuum level (below 10^{-7} Torr) until the level of H atoms produced in the blank test of shock heated pure Ar falls down below the detection limit. Also, blank tests for H and O atoms by ARAS have been carefully conducted so as to confirm that the contributions of the background H and/or O atoms from impurities produced in H_2/Ar and O_2/Ar mixtures are negligible. In addition, measurements for the title reaction have been repeated at least two times for all the shock conditions to retain the reliability.

Sample mixtures of 0.2/0.4 ppm CH_2I_2 +100/262 ppm O_2 and 0.2/0.4 ppm CH_2I_2 +300 ppm H_2 diluted in Ar are prepared simply by the measurement of pressure by using a combination of Baratron pressure gauges. These CH_2I_2/H_2 and CH_2I_2/O_2 samples were prepared by introducing the same partial pressure of CH_2I_2 into the separate sample cylinders at the same time so as to ensure the concentration of CH_2I_2 through the comparative measurements, as demonstrated in the following section. The initial concentration of CH_2I_2 can be re-evaluated by analyzing the evolution of H atoms produced in the mixture of CH_2I_2 + 300 ppm H_2. Conducting all these additional experimental procedures is actually time-consuming, but such careful examination should be essential to guarantee the reliability when the concentration of the test gas is extremely low.

He (99.9995%, AGA Specialty Gases) and Ar (99.9995%, AGA Specialty Gases), H_2 (99.9995%, AGA Specialty Gases), O_2 (99.995%, Scott Specialty Gases), and N_2O (99.999%, Scott Specialty Gases) are used without further purification. CH_2I_2 (99%, Sigma-Aldrich, Reagent Plus grade) and C_2H_5I (99%, Sigma-Aldrich, Reagent Plus grade) are purified by repeating degassing by successive freezing and pumping cycles.

3. EXPERIMENTAL RESULTS

The experimental condition is summarized in Table 1. Evolutions of H and O atoms are monitored in the temperature range 1850−2050 K: The lower limit of the temperature range is chosen so that the thermal decomposition of CH_2I_2 is sufficiently fast enough to evaluate the rates and the branching fractions of the reaction $^{1,3}CH_2 + O_2 \rightarrow$ products (reactions 2 and 3), without having too large uncertainty, and the upper limit is to avoid the influence of the thermal decomposition of CH_2O, which is expected to be one of the possible products of reactions 2 and 3.

The evolutions of [H] observed in the mixtures of 0.2 ppm CH_2I_2 + 100 ppm O_2 and 0.2 ppm CH_2I_2 + 300 ppm H_2 are demonstrated in Figure 2.

For the sample of 0.2 ppm CH_2I_2 + 100 ppm O_2, the evolution of [H] shows rapid initial increase then followed by slower decay due to the consumption by H + $O_2 \rightarrow$ OH + O (reaction 5). By contrast, the profile of [H] in the mixture of 0.2 ppm CH_2I_2 + 300 ppm H_2 appears to keep increasing, exceeding the initial concentration of CH_2I_2 because CH_3 produced in reactions 6 or 7 can generate another H atom through reaction 8, i.e.,

$$^{3}CH_2 + H_2 \rightarrow CH_3 + H \quad (6)$$

$$^{1}CH_2 + H_2 \rightarrow CH_3 + H \quad (7)$$

$$CH_3 + H_2 \rightarrow CH_4 + H \quad (8)$$

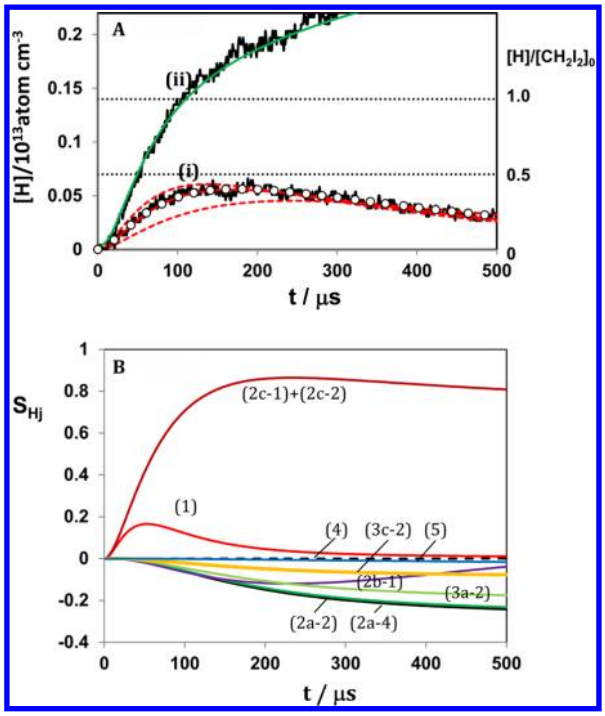

Figure 2. Comparison of the evolutions of H atoms produced in the 0.2 ppm CH_2I_2 + 100 ppm O_2 and 0.2 ppm CH_2I_2 + 300 ppm H_2 diluted in Ar (A), and the sensitivity analysis for H atom (B). (A) (i): 0.2 ppm CH_2I_2 + 100 ppm O_2 in Ar, T = 2005 K, P = 1.91 atm, [Ar] = 7.0×10^{18}/cm^3, [O_2] = 7.0×10^{14}/cm^3, [CH_2I_2]$_0$ = 1.40×10^{12}/cm^3. Observed evolutions of H atom (shown by the black solid line) is compared with kinetic simulations using the analytical solution of (II) (red solid curve with k_2'/cm^3 molecule^{-1} s^{-1} = 1.94×10^{-11}), and the numerical solution using the reaction scheme of Table 2 (black circle). The two red dashed curves are the solutions of (II) with $1.5k_2'$ and $0.5k_2'$. (ii): 0.2 ppm CH_2I_2 + 300 ppm H_2 in Ar, T = 2005 K, P = 1.91 atm, [Ar] = 7.0×10^{18}/cm^3, [H_2] = 2.1×10^{15}/cm^3, [CH_2I_2]$_0$ = 1.40×10^{12}/cm^3. The result of the kinetic simulation is shown by the green solid curve. (B) The sensitivity coefficients for H atom, defined by $S_{Hj} = \partial Y_H / \partial[\ln k_j]$, where Y_H is the mass fraction of H atom, and the labeled reaction number j is shown in Table 2 as well as in the text.

Clearly, the profile of [H] in this case is very sensitive to the initial concentration of CH_2I_2 (or CH_2). As shown by the green solid curve (ii) in Figure 2, evolution of [H] by the numerical computation based on the reaction scheme of Table 2 agrees very well with the observed profile of [H] by using reasonable rates for 6 and 7.[28,34,35] Such comparative measurement appears to guarantee the assigned initial concentration of CH_2I_2 (denoted as [CH_2I_2]$_0$) assigned from the pressure measurement.

In the numerical computation of the evolutions of [H] and [O] atoms, it is practically impossible to find out an optimized combination of the rate parameters for the complicated reaction system associated with multiple reaction channels only from the experimental information of [H] and [O] atoms; therefore, the present analysis has been based on the simplified reaction schemes 2a−2c and 3a−3c.

The evolutions of [H] and [O] can be analyzed by taking only reactions 1−5 into account, since the concentration of CH_2I_2 is very low in this study; i.e., [CH_2I_2]$_0$ = (1−4) × 10^{12} molecule/cm^3, and the contributions of the secondary reactions should be negligibly small.

dx.doi.org/10.1021/jp307140z | J. Phys. Chem. A 2012, 116, 9245−9254

Table 2. The Reaction Scheme Employed for the Simulations of CH_2I_2+O_2 and CH_2I_2+H_2 Reactions

	reactions[a]	A^a	n^a	Θ^a	reference
1	$CH_2I_2 + Ar \rightarrow {}^3CH_2 + 2I + Ar$	3.12×10^{-8}	0	30170	28
2a-2	${}^3CH_2 + O_2 \rightarrow H + OH + CO$		see text		[b]
2a-4	${}^3CH_2 + O_2 \rightarrow 2H + CO_2$		see text		[b]
2b-1	${}^3CH_2 + O_2 = O + CH_2O$		see text		
2c-1	${}^3CH_2 + O_2 = H_2 + CO_2$		see text		[c]
2c-2	${}^3CH_2 + O_2 = H_2O + CO$		see text		[c]
3a-2	${}^1CH_2 + O_2 = H + OH + CO$	4.65×10^{-11}	0	0	18
3c-2	${}^1CH_2 + O_2 = H_2O + CO$	1.99×10^{-11}	0	0	18
4	${}^1CH_2 + Ar = {}^3CH_2 + Ar$	1.50×10^{-11}	0	302	18
5	$H + O_2 = OH + O$	1.62×10^{-10}	0	7475	18
6	${}^3CH_2 + H_2 = H + CH_3$	7.33×10^{-19}	2.3	3699	32
7	${}^1CH_2 + H_2 = CH_3 + H$	1.26×10^{-10}	0	0	28
8	$CH_3 + H_2 = CH_4 + H$	1.49×10^{-20}	2.7	4740	18
9	$O + H + Ar = OH + Ar$	5.81×10^{-7}	−1	0	18
10	$2O + Ar = O2 + Ar$	1.40×10^{-7}	−1	0	18
11	$2H + Ar = H_2 + Ar$	1.05×10^{-6}	−1	0	18
12	$CH_3 + O_2 = O + CH_3O$	5.91×10^{-11}	0	15347	18
13	$CH_3 + O_2 = OH + CH_2O$	3.84×10^{-12}	0	10229	18
14	$OH + H_2 = H_2O + H$	3.59×10^{-16}	1.51	1727	18
15	$OH + OH = O + H_2O$	1.23×10^{-21}	−0.37	0	18
16	$CH_3 + OH = {}^1CH_2 + H_2O$	1.07×10^{-6}	−1.34	713	18
17	$CH_3 + OH = {}^3CH_2 + H_2O$	9.30×10^{-17}	1.6	2725	18
18	${}^3CH_2 + OH = CH_2O + H$	3.32×10^{-11}	0	0	18
19	$2CH_3(+Ar) = C_2H_6(+Ar)$	6.77×10^{-16}	−1.18	329	18
20	$CH_3 + CH_3 = C_2H_5 + H$	1.14×10^{-11}	0.1	5337	18
21	$CH_3 + {}^3CH_2 = C_2H_4 + H$	6.64×10^{-11}	0	0	18
22	$H + C_2H_3(+Ar) = C_2H_4(+Ar)$	6.08×10^{-12}	0.27	141	18
23	${}^3CH_2 + {}^3CH_2 = H_2 + C_2H_2$	2.66×10^{-9}	0	6014	18
24	$CH_3 + O = CH_2O + H$	8.41×10^{-11}	0	0	18
25	$CH_3 + O = H_2 + CO + H$	5.60×10^{-11}	0	0	18
26	$O + H_2 = OH + H$	6.43×10^{-20}	2.7	3152	18
27	$CH_2O + H(+)AR \cong CH_2OH + AR$	8.97×10^{-13}	0.454	1813	18
28	$CH_2O + H + AR = CH_3O + AR$	8.97×10^{-13}	0.454	1309	18
29	$CH_2O + H + AR = CH_3O + AR$	1.81×10^{-12}	0.48	−131	18
30	$H_2 + CO + AR = C\,H_2O + AR$	7.14×10^{-17}	1.5	40080	18
31	$HCO + Ar = H + CO + Ar$	3.11×10^{-7}	−1.0	85600	18
32	$C_2H_4 + H + Ar = C_2H_5 + Ar$	8.97×10^{-13}	0.454	916	18
33	$C_2H_2 + H + Ar = C_2H_3 + Ar$	6.51×10^{-12}	0	1208	18
34	$CH_2O + OH = H_2O + HCO$	5.70×10^{-15}	1.18	−225	18
35	$CH_2O + CH_3 = CH_4 + HCO$	5.51×10^{-21}	2.81	2951	18
36	$CH_2O + H = H_2 + HCO$	9.53×10^{-17}	1.9	1381	18
37	$CH_2O + O = OH + HCO$	6.48×10^{-11}	0	1782	18
38	${}^3CH_2 + {}^3CH_2 \rightarrow 2H + C_2H_2$	3.32×10^{-10}	0	5533	18
39	$HO_2 + OH = H_2O + O_2$	2.41×10^{-11}	0	−252	18
40	$H + O_2 + Ar = O_2 + Ar$	1.16×10^{-6}	−0.8	0	18

dx.doi.org/10.1021/jp307140z | J. Phys. Chem. A 2012, 116, 9245−9254

Table 2. continued

	reactions[a]	A^a	n^a	Θ^a	reference
41	$H + O_2 + Ar = O_2 + Ar$	1.66×10^{-12}	0	0	18
42	$HO_2 + CH_3 = CH_3O + OH$	6.28×10^{-11}	0	0	18
43	$H + HO_2 = H_2 + O_2$	7.44×10^{-11}	0	538	18
44	$H + HO_2 = O + H_2O$	6.59×10^{-12}	0	338	18
45	$H + HO_2 = 2OH$	1.40×10^{-10}	0	320	18
46	$O + HO_2 = OH + O_2$	3.32×10^{-11}	0	0	18
47	$^3CH_2 + HO_2 = CH_2O + OH$	3.32×10^{-11}	0	0	18
48	$CH_3 + C_2H_6 = CH_4 + C_2H_5$	5.88×10^{-18}	2.1	438	18
49	$OH + C_2H_6 = H_2O + C_2H_5$	1.02×10^{-17}	1.7	5262	18
50	$H + C_2H_6 = H_2 + C_2H_5$	1.91×10^{-16}	1.92	3792	18
51	$O + C_2H_6 = OH + C_2H_5$	1.49×10^{-16}	1.92	2865	18

[a]The reverse reaction is considered when the reactants and the products are connected by " = ". The rate is expressed by $k = AT^n \exp(-\Theta/T)$ in units of cm^3, molecule, s, and K. [b]In conducting numerical simulation, $^3CH_2 + O_2 \rightarrow HCO + CO$ 2a-1) and $^3CH_2 + O_2 \rightarrow H + HOCO$ (2a-3) are represented by 2a-2 and 2a-4, respectively. Any combination of $k_{2a\text{-}2}$ and $k_{2a\text{-}4}$ gives the same calculated profiles of H and O if $k_{2a\text{-}2} + 2k_{2a\text{-}4}$ is kept constant for the present experimental condition. [c]Any combination of $k_{2c\text{-}1}$ and $k_{2c\text{-}2}$ gives the same calculated profiles of H and O as long as $k_{2c\text{-}1} + k_{2c\text{-}2}$ is kept constant for the present experimental condition.

With an approximation of the quasi-equilibrium between $[^1CH_2]$ and $[^3CH_2]$, i.e., $[^1CH_2]/[^3CH_2] = Kc_4$ (Kc_4 is the equilibrium constant of reaction 4), the analytical solutions can be given as

$$[^3CH_2]/[CH_2I_2]_0 = [R_1/(R_2' - R_1)/(1 + Kc_4)] \times [\exp(-R_1t) - \exp(-R_2't)] \quad (I)$$

$$[H]/[CH_2I_2]_0 = [\phi_{2a}'R_1R_2'/(R_2' - R_1)] \times \{[\exp(-R_1t) - \exp(-R_5t)] /(R_5 - R_1) - [\exp(-R_2't) - \exp(-R_5t)] /(R_5 - R_2')\} \quad (II)$$

$$[O]/[CH_2I_2]_0 = [R_1R_2'/(R_2' - R_1)] \times [\phi_{2b}'F_1 + \phi_{2a}'R_5(F_2 - F_3)] \quad (III)$$

where

$F_1 = [1 - \exp(-R_1t)]/R_1 - [1 - \exp(-R_5t)]/R_5$,
$F_2 = \{[1 - \exp(-R_1t)]/R_1 - [1 - \exp(-R_5t)]/R_5\}/(R_5 - R_1)$,
$F_3 = \{[1 - \exp(-R_2't)]/R_2' - [1 - \exp(-R_5t)]/R_5\}/(R_5 - R_2')$.
$R_1 = k_1[Ar]$, $k_2' = k_2(1 + \alpha)/(1 + Kc_4)$, $R_2' = k_2'[O_2]$, $R_5 = k_5[O_2]$,
$\phi_{2a} = k_{2a}/k_2$, $\phi_{2b} = k_{2b}/k_2$, $\phi_{3a} = k_{3a}/k_3$, $\phi_{3b} = k_{3b}/k_3$,
$\phi_{2a}' = (\phi_{2a} + \alpha\phi_{3a})/(1 + \alpha)$, $\phi_{2b}' = (\phi_{2b} + \alpha\phi_{3b})/(1 + \alpha)$, and $\alpha = (k_3/k_2)Kc_4$.

Although the above analytical solution formally corresponds only to the reaction channels of a single H atom formation, i.e., $CH_2 + O_2 \rightarrow H +$ products (reactions2a-1, 2 and 3a-1, 2), the channels of producing two H atoms, i.e., $CH_2 + O_2 \rightarrow 2H +$ products (reactions 2a-3, 4 and 3a-3, 4) can be also included, for instance, by defining the branching fractions as, $\phi_{2a} = (\phi_{2a\text{-}2} + 2\phi_{2a\text{-}4})$ and $\phi_{3a} = (\phi_{3a\text{-}2} + 2\phi_{3a\text{-}4})$.

By fitting the solutions of eqs II and III to the experimentally observed [H] and [O] profiles, it is possible to evaluate k_2', ϕ_{2a}', and ϕ_{2b}', where the rates for reactions 1 and 5 are supplied from previous studies.[28,18] The physical-chemical meanings of these parameters are the effective reaction rate and the branching fractions of producing H and O atoms in the reaction of $CH_2 + O_2$, respectively, under the quasi-equilibrium condition in between $^3CH_2$ and $^1CH_2$.

In the analysis of [H], k_2' as well as ϕ_{2a}' are evaluated by using eq II so that the normalized deviation of analytical solution from experimental profile becomes minimum. An example of such analysis is shown by the red solid curve in Figure 2A; excellent agreement is attained in the evolution of H atoms for all the experimental data.

Also, the experimental profiles of O atoms for the mixtures of 0.2−0.4 ppm CH_2I_2 + excess O_2 are used to evaluate k_2', ϕ_{2a}', and ϕ_{2b}', although the S/N ratio is about 1/3 of that for H atoms. As shown in Figure 3A, in contrast to [H], the evolution of [O] exhibits consistent increments exceeding the maximum concentration of H atoms. The profile of O atoms reflects that additional conversion of H to O atoms through the reaction $H + O_2 \rightarrow OH + O$ (5) is imposed on the initial production of O by reactions 2 and 3, i.e., the asymptote of [O] to $t = \infty$ should correspond to $\phi_{2a}' + \phi_{2b}'$. In the practical data analysis for [O], optimized conditions are searched for the three parameters (R_2', ϕ_{2a}', and ϕ_{2b}') by conducting iteration of computation until the normalized deviation of the solution of eq III from experimental data is minimized. An example of the analytical solution is shown in Figure 3A by the red solid curve: reasonable agreement with the observed evolution of O atoms has been attained for all the data of this study.

The results of the numerical computation using 51 elementary reactions, given in Table2,[18,28,36] are shown by the black circles in Figures 2A and 3A; excellent agreement of the numerical solutions with the analytical solutions is attained for both H and O atoms. The sensitivity analysis for the profiles of H and O atoms has been also conducted using the reaction scheme of Table 2, and examples are demonstrated in Figures 2B and 3B, respectively. It is confirmed that the reactions other than 1, 2, 3, and 5 exhibit very small sensitivity. Although the reaction scheme employed in Table 2 has not been optimized for the present experimental conditions, it was also prepared for the experiment using a higher concentration of CH_2 to afford measurement of the production yield of CO, which is much less sensitive than H and O atoms. Validity of the reaction scheme and kinetic

dx.doi.org/10.1021/jp307140z | J. Phys. Chem. A 2012, 116, 9245−9254

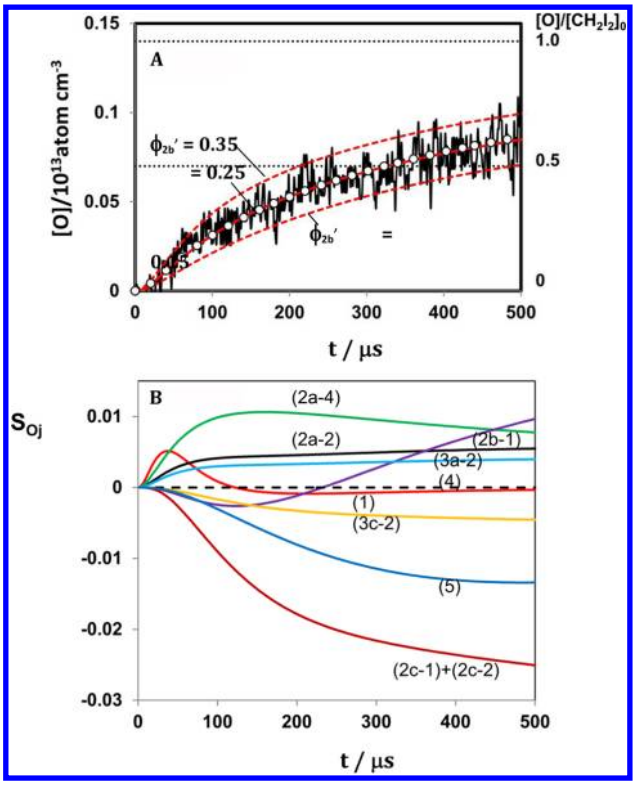

Figure 3. An example of the evolution of O atoms produced in a highly diluted $CH_2I_2 + O_2$ mixture. Sample gas: 0.2 ppm CH_2I_2 + 100 ppm O_2 in Ar, T = 2005 K, P = 1.91 atm, [Ar] = 7.0×10^{18}/cm^3, $[CH_2I_2]_0 = 1.40 \times 10^{12}$/cm^3. (A) Observed evolution of O atom (shown by the black solid line) is compared with kinetic simulations using the analytical solution of eq III (red solid curve with $\phi_b' = 0.25$), and the numerical solution using the reaction scheme of Table 2 (black circle). The two red dashed curves are the solutions of (III) with $\phi_b' = 0.35$ and 0.15. (B) The sensitivity coefficients for O atom, defined by $S_{Oj} = \partial Y_O/\partial[\ln k_j]$, where Y_O is the mass fraction of O atom, and the labeled reaction number j is shown in Table 2 as well as in the text.

parameters given in Table 2 will be examined in the extended work.

By conducting calculations concerning experimental uncertainties, it is confirmed that the experimental error of k_1 reported in the original study[28] does not influence the evaluated k_2', ϕ_{1a}', nor ϕ_{1b}', since the experimental conditions have been chosen so that the profiles of H and O atoms are sensitive mainly to the rates and branching fractions of reactions 2 and 3, as well as 5. It is also confirmed that the decaying part of the profile of H atoms and the corresponding increment of O atoms followed by the initial production by reactions 2 and 3 can be very well explained by using a single rate expression for the reaction[18] H + O_2 → OH + O (5); very small uncertainty for the evaluated k_2', ϕ_{1a}', or ϕ_{1b}', if any, will be induced by the uncertainty of the rate of reaction 5.

The result of the analysis on k_2' [$=k_2(1 + \alpha)/(1 + Kc_4)$] is summarized in Figure 4 as well as in Table 1. Magnitudes of k_2' evaluated independently from the profiles of H and O atoms are found to be consistent each other; all the measured rates can be summarized as k_2'/cm^{3}molecule^{-1} s^{-1} = $(1.90 \pm 0.31) \times 10^{-11}$ (T = 1850−2050 K) without obvious temperature dependence.

The parameter α represents the relative magnitude of the contribution of $^1CH_2 + O_2$ (3) against $^3CH_2 + O_2$ (2) in the reaction of $CH_2 + O_2$; it is possible to evaluate α by employing the experimental result on k_3 given in the previous experimental studies at room temperature assuming that k_3 has no tempera-

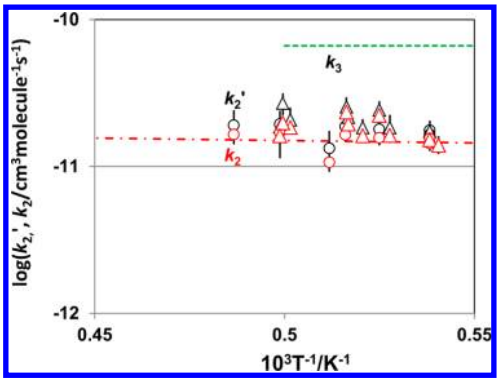

Figure 4. Summary of the reaction rate for $CH_2 + O_2$ → products (k_2'), and $^3CH_2 + O_2$ → products (k_2), obtained in the present study. The experimental results of this study on k_2' are expressed by the black symbols, where ○ = evaluated by the evolution of [H] and Δ = evaluated by the evolution of [O], and k_2 is expressed by the red symbols, where ○ = evaluated by the evolution of [H] and Δ = evaluated by the evolution of [O]. Extrapolation of the reported k_2 at low temperature range (ref 21) is given by the dash-dotted line; also k_3 (ref 18) is shown by the dashed green line for comparison.

ture dependence. The removal rate (reaction 3 + collisional quenching (4)] is reported to be 3×10^{-11} cm^3 molecule^{-1} s^{-1} at 298 K by Ashford et al.[26] This is substantially smaller than the result of 7.4×10^{-11} cm^3 molecule^{-1} s^{-1} measured by Langford et al. at 295 K.[27]

GRI-mech 3.0 employs the rate for reaction 3 based on the latter study, but the correction for the contribution of reaction 4 has been added, i.e., k_3 is given as 6.64×10^{-11} cm^3 molecule^{-1} s^{-1} (independent of temperature), and the evaluation of the parameter $\alpha = (k_3/k_2)Kc_4$ in this study has been conducted based on this rate. The result on α is summarized in Figure 5; the magnitude of α is indicated to be $\alpha = 0.18 \pm 0.04$. This means that the contribution of $^1CH_2$ on the measured rate of k_2' [given by $\alpha/(1 + \alpha)$] is only about 15% (if the result of k_3 reported by Ashford et al.[18] is employed, the contribution of $^1CH_2$ is less than 10%); i.e., the measured k_2' approximately represents the rate of reaction 2. The result on k_2 is summarized in Table 1 and Figure 4 compared with k_2'; as a summary, the reaction rate for reaction 2 can be expressed by k_2/ cm^3 molecule^{-1} s^{-1} = $(1.69 \pm 0.31) \times 10^{-11}$ (T = 1850−2050 K).

The present results on k_2' and k_2 are compared with the previous works in Figure 6. The result of the previous study at high temperature range (1000 − 1700 K)[23,25] is found to be about an order of magnitude lower than the result of this study. Although the reason for having such disagreement between the results on k_2 obtained in the previous and the present works is not clear, contributions of the secondary reactions may be too large in the previous study to evaluate k_2 accurately. It is also indicated that extrapolation of k_2 measured by Vinckler and Debruyn with a mass-spectrometric technique over 295−600 K[21] agrees very well with this study.

Combination of the result on k_2 at low temperature given by Vinckler and Debruyn with the present data may be recommendable as the database in combustion modeling over a wide temperature range, i.e.,

$$k_2/\text{cm}^3\ \text{molecule}^{-1}\ \text{s}^{-1} = 2.74 \times 10^{-11}\exp(-874/T),\ (T = 295-2050\text{K}) \quad \text{(IV)}$$

The results of the measurement of the branching fractions ϕ_{2a}' and ϕ_{2b}' are summarized in Figure 7 and in Table 1. As for the yield of production of H atoms, the magnitudes of ϕ_{2a}' analyzed

dx.doi.org/10.1021/jp307140z | J. Phys. Chem. A 2012, 116, 9245−9254

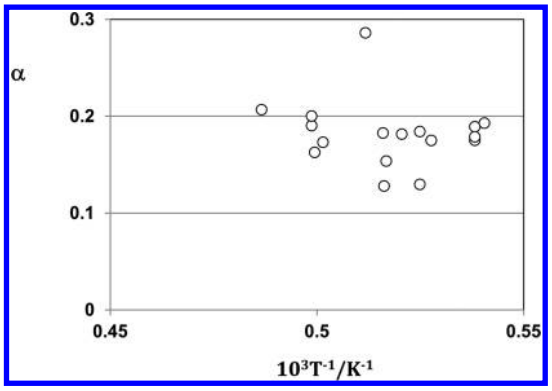

Figure 5. Summary of the evaluated parameter α. The parameter α [relative contributions of $^1CH_2$ and $^3CH_2$ in the reaction of $CH_2 + O_2$ defined as $\alpha = (k_3/k_2)Kc_4$] evaluated in this study is expressed by the black circle (see text).

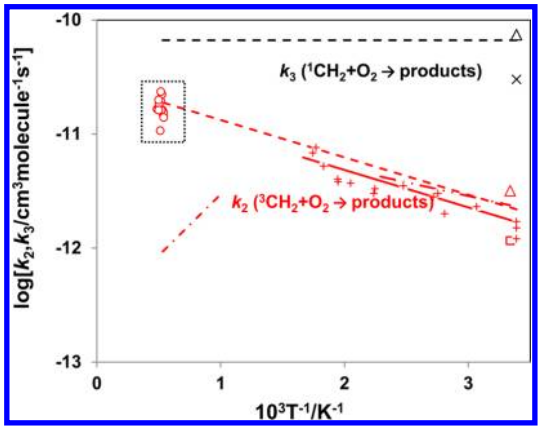

Figure 6. Arrhenius plot of the reaction rate for $^3CH_2 + O_2 \rightarrow$ products (k_2), and $^1CH_2 + O_2 \rightarrow$ products (k_3). k_2 is expressed by red symbols, where ○ = present study, Δ = ref 20, □ = ref 22, + and solid line = ref 21, dash-dot line = ref 24, dash-dot-dot line = ref 23, and dashed line = ref 18. k_3 is expressed by the black symbols, where × = ref 26, Δ = ref 27, and dashed line = ref 18.

from the evolutions of [H] and [O] are found to be consistent each other. In order to estimate ϕ_{2a} and ϕ_{2b} from the present results of ϕ_{2a}' and ϕ_{2b}', it is necessary to assign the branching fractions of reaction 3 (i.e., ϕ_{3a} and ϕ_{3b}) in addition to α, but no information is available for these branching fractions.

It may be worth mentioning that $\phi_{2a} \cong \phi_{2a}'$ and $\phi_{2b} \cong \phi_{2b}'$ if the product branching fraction for reaction 3 is approximately the same as that for reaction 2, i.e., $\phi_{3a} \cong \phi_{2a}$, and $\phi_{3b} \cong \phi_{2b}$, respectively. Even if the product branching fractions for reactions 2 and 3 are very much different each other, only a small correction is required in converting ϕ_{2a}' to ϕ_{2a}, as well as ϕ_{2b}' to ϕ_{2b}, since the contribution of $^1CH_2$ is minor. As an example, the results of the analysis on ϕ_{2a} and ϕ_{2b} by using the branching fractions proposed in GRI-mech 3.0 ($\phi_{3a} = 0.7$ and $\phi_{3b} = 0$)[18] are shown in Table 1 and Figure 7. The difference of the estimated ϕ_{2a}' and ϕ_{2a}, as well as ϕ_{2b}' and ϕ_{2b} is not large. It would be appropriate to consider that the branching fractions for reaction 2 are given approximately by averaging ϕ_{2a} and ϕ_{2a}' shown in Table 1, as well as ϕ_{2b} and ϕ_{2b}', even though reliable information on the magnitudes of ϕ_{3a} and ϕ_{3b} is not available.

As a result of such analysis, the net branching fractions for producing H and O atoms in the $^3CH_2$+O_2 reaction are given as $\phi_{2a} = 0.58 \pm 0.06$ and $\phi_{2b} = 0.25 \pm 0.06$, where no obvious

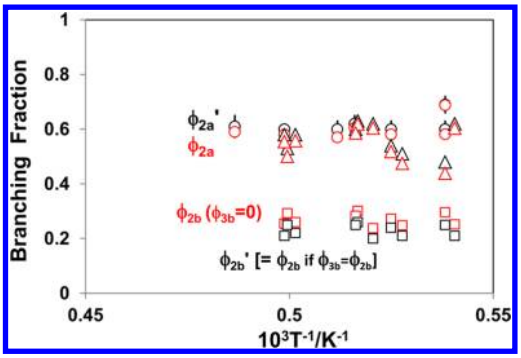

Figure 7. Summary of the measured branching fractions for the reaction $CH_2 + O_2 \rightarrow H +$ products, and $CH_2 + O_2 \rightarrow O +$ products. Branching fraction for producing H atom: ϕ_{2a}' (black symbols) and ϕ_{2a} (red symbols); ○ = determined by the evolution of H atom, Δ = determined by the evolution of O atom. Branching fraction for producing O atom, ϕ_{2b}' and ϕ_{2b}: □ = determined by the evolution of O atom. The black square denotes ϕ_{2b}' corresponding to the reactions $^{1,3}CH_2 + O_2$ (2, 3) [$\phi_{2b}' = \phi_{2b}$ if $\phi_{2b} = \phi_{3b}$]. The red square denotes ϕ_{2b} with the branching fraction $\phi_{3b} = 0$ (ref 18).

temperature dependence is indicated. In addition, the asymptote of $[O]/[CH_2I_2]_0$ for large t (which should correspond approximately to $\phi_{2a} + \phi_{2b}$) is confirmed to be 0.8 − 0.9 for the measurements in the highest concentration of O_2 (262 ppm). This would also support the validity of the evaluated branching fractions in this study.

4. DISCUSSIONS

It is clearly demonstrated that H and O atoms are the main products of reactions 2 and 3; the sum of the yields of H and O atoms produced in reactions 2 and 3 is shown to be 80 −90% of initial CH_2. Because the contribution of $^1CH_2$ is minor in the evaluated branching fractions as is shown above, it may be reasonable to focus only to the reaction $^3CH_2 + O_2$ (2), for simplicity, in the following discussion.

Most of the previous theoretical works discussed only the reaction channels for producing stable molecules such as $CO_2 + H_2$ or $CO + H_2O$.[12,13,37] As the reaction is highly exothermic, internally hot reaction intermediates are produced, and the dynamic effect in the product branching should be important; such a nonequilibrium treatment of the reaction systems increases the difficulty in estimating the branching fractions of the products. Due to the interest to the atmospheric chemistry, extensive studies on the ozonolysis of alkenes and structures of carbonyl oxides and their isomers have been conducted to clarify the reaction mechanism.[1−10,38−43] Direct production of OH and $O(^3P)$ was reported in the experimental studies in the ozonolysis of ethene. Strong pressure dependence on the production yield of OH was reported in the reaction of $O_3 + C_2H_4$; the yield is 0.2 at 1 atm air, but increases to 0.42 at 5.5 Torr.[16] Production of 0.01−0.05 of $O(^3P)$ was indicated in the reaction of $^3CH_2 + O_2$ at room temperature and 1 atm in another study.[38] Theoretical calculations have been conducted to evaluate the branching fractions of producing OH[42] and $O(^3P)$[43] in the reactions of $C_2H_4 + O_3$ including the reaction pathway of CH_2O_2. Even though the contribution of the excited state is taken into consideration by using the master equation and statistical theory, much lower production yields for OH (~0.2%) than those observed in the experimental studies were indicated;[42] however, production yield of OH from excited CH_2O_2 formed in the reaction of $^3CH_2 + O_2$ can be much higher than that of the

dx.doi.org/10.1021/jp307140z | J. Phys. Chem. A 2012, 116, 9245−9254

$C_2H_4 + O_3$ reaction since the former reaction is 20 kcal/mol more exothermic.

The reaction mechanism for the unimolecular decomposition of formic acid (reactions 9) was studied by calculating potential energy surfaces using a quantum-chemical analysis.[11,37] Computation by the high-level G2M(CC1) method and microcanonical RRKM theory indicates that two reaction pathways, 9a and 9b, were suggested to dominate other reaction channels:[37]

$$HCOOH \rightarrow CO + H_2O \quad (9a)$$

$$\rightarrow CO_2 + H_2 \quad (9b)$$

It is also indicated that 9a is far more probable than 9b, i.e., k_{9a}/k_{9b} = 13.6−13.9 between 1300 and 2000 K.

The present experimental result on the branching fraction for producing H and O atoms indicates that the production of H_2 + CO_2 in reaction 2c-1 or H_2O + CO (2c-2) cannot be the dominant reaction channels in reaction 2, i.e., the branching for the products containing H and O atoms cannot be explained by the simple unimolecular behavior in the HCOOH decomposition (reactions 9). The branching fractions for the production channels of CO_2 and CO in reaction 2 measured by IR diode laser absorption at room temperature[31] are also inconsistent with those measured by the unimolecular decomposition of HCOOH.

Although the yields of products may have temperature dependence, it is interesting to compare the branching fractions of CO, CO_2, and CH_2O measured at room temperature[31] with the present result on the branching fractions for H and O atoms.

As for the production channel of O atoms, it is indicated that O atoms are produced from the surface crossing from the singlet to triplet states of the isomers of CH_2OO; the counterpart of the product $O(^3P)$ is CH_2O, i.e., $^3CH_2 + O_2 \rightarrow CH_2O + O(^3P)$ (reaction 2b-1) is supposed to be dominant for the production of O atoms.[41] The branching fraction for $O(^3P)$ atoms production (0.25 ± 0.06) given in this study appears to be slightly larger than that for CH_2O (0.16 ± 0.04.) reported by the IR diode laser absorption measurement at room temperature;[31] however, they overlap each other if the error limits are taken into consideration.

As for the production of H atoms, channels 2a-1−2a-4 correspond to reaction 2a, because HCO and HOCO should decompose immediately at high temperature leading to the formation of H + CO and H + CO_2; it is not necessary in this study to consider the contributions of the reactions HCO + O_2 or HOCO + O_2.[44,45] If H atoms are mainly produced from highly excited HCOOH (as drawn by the dotted lines in Figure 1), it may be reasonable to assume that reactions 2a-1 and/or (2a-3 are the candidates of the main channels for the production of H atoms by simply breaking C−OH and/or C−H bonds in HCOOH, leading to the formation of OH + HCO (2a-1) and H + HOCO (2a-3), respectively. The yields of H atoms measured in this study and those of CO and CO_2 measured in the IR diode laser absorption can be consistent by assigning approximately the same magnitudes to all the branching fractions for the product channels: H + OH + CO (2a-1 or 2a-2), 2H + CO_2 (2a-3 or 2a-4), H_2 + CO_2 (2c-1) and H_2O + CO (2c-2), i.e., $\phi_{2a\text{-}1}$ (or $\phi_{2a\text{-}2}$) $\cong \phi_{2a\text{-}3}$ (or $\phi_{2a\text{-}4}$) $\cong \phi_{2c\text{-}1} \cong \phi_{2c\text{-}2} = 0.2 \pm 0.05$. This may indicate that no special product channel dominates in the reaction $^3CH_2 + O_2$ (2). As a substantial difference exists among the barrier heights and the heats of formation for these reaction channels, such nonselectivity may be due to the dominance of the reactions of highly excited reaction intermediates even for the relatively high pressure condition (about 2 atm) of this study.

Of course, the above discussion is too simple and primitive for explaining the reaction mechanism of reaction 2. In order to explain the present result on H and $O(^3P)$ as main products of reaction 2, detailed theoretical examination of the reactions of highly excited intermediates would be desirable, even if the reaction system may be too complicated for evaluating the product branching quantitatively.

AUTHOR INFORMATION

Corresponding Author

*E-mail: Niann-Shiah Wang: nswang@nctu.edu.tw (N.-S.W.); matsui@tut.ac.jp (H.M.).

Notes

The authors declare no competing financial interest.

ACKNOWLEDGMENTS

This work was supported by the National Science Council of Taiwan under Grant No. NSC 100-2113-M-009-007. H.M. deeply acknowledges the supports by National Science Council of Taiwan and National Chiao Tung University.

REFERENCES

(1) Ha, T.-K.; Kühne, H.; Vaccani, S.; Güenthard, Hs. H. *Chem. Phys. Lett.* **1974**, *24*, 172−174.
(2) Criegee, R. *Angew. Chem., Int. Ed. Engl.* **1975**, *14*, 745−752.
(3) Harding, L. B.; Goddard, W. *J. Am. Chem. Soc.* **1978**, *100*, 7180−7188.
(4) Karlström, G.; Engström, S.; Jönsson, B. *Chem. Phys. Lett.* **1979**, *67*, 343−347.
(5) Cremer, D.; Schmidt, T.; Gauss, J.; Radbakrishnan, T. P. *Angew. Chem., Int. Ed. Engl.* **1988**, *27*, 427−428.
(6) Bach, R. D.; Andres, J. L.; Owensby, A. L.; Sclegel, H. B.; McDouall, J. J. W. *J. Am. Chem. Soc.* **1992**, *114*, 7207−7217.
(7) Karistrom, G.; Roos, B. O. *Chem. Phys. Lett.* **1981**, *79*, 416−420.
(8) Cimiraglia, R.; Ha, T.-K.; Günthard, Hs. H. *Chem. Phys. Lett.* **1982**, *85*, 262−265.
(9) Dupuis, M.; Lester, W. A. *J. Chem. Phys.* **1984**, *80*, 4193−4195.
(10) Goddard, J. D.; Yamaguchi, Y.; Schaefer, H. F. *J. Chem. Phys.* **1992**, *96*, 1158−1166.
(11) Francisco, J. S. *J. Chem. Phys.* **1992**, *96*, 1167−1175.
(12) Anglada, J. M.; Bofill, J. M.; Olivella, S.; Solé, A. *J. Phys. Chem. A* **1998**, *102*, 3398−3406.
(13) Chen, B.; Huang, M.; Su, H.; Kong, F. *Acta Phys. Chim. Sin.* **2000**, *16*, 869−872.
(14) Gutbrod, R.; Kraka, E.; Schindler, R. N.; Cremer, D. *J. Am. Chem. Soc.* **1997**, *119*, 7330−7342.
(15) Horie, O.; Moortgat, G. K. *Acc. Chem. Res.* **1998**, *31*, 387−396.
(16) Fenske, G. D.; Hasson, A. S.; Paulson, S. E.; Kuwata, K. T.; Ho, A.; Houk, K. N. *J. Phys. Chem. A* **2000**, *104*, 7821−7833.
(17) Warnatz, J. In *Combustion Chemistry*; Gardiner, W.C., Ed.; Springer-Verlag: New York, 1984; Chapter 5.
(18) Smith, G. P.; Golden, D. M.; Frenklach, M.; Moriarty, N. W.; Eiteneer, B.; Goldenberg, M.; Bowman, C. T.; Hanson, R. K.; Song, S.; Gardiner, W. C., Jr.; Lissianski, V. V.; Qin, Z. http://www.me.berkeley.edu/gri mech.
(19) Andersen, A.; Carter, E. A. *J. Phys. Chem. A* **2003**, *107*, 9463−9478.
(20) Pilling, M. J.; Robertson, J. A. *J. Chem. Soc., Faraday Trans. 1* **1977**, *73*, 968−984.
(21) Vinckler, C.; Debruyn, W. *J. Phys. Chem.* **1979**, *83*, 2057−2062.
(22) Darwin, D. C.; Young, A. T.; Johnston, H. S.; Moore, C. B. *J. Phys. Chem.* **1989**, *93*, 1074−1078.
(23) Dombrowsky, Ch.; Hwang, S. M.; Rohrig, M.; Wagner, H.Gg. *Ber. Bunsenges. Phys. Chem.* **1992**, *96*, 194−198.
(24) Bley, U.; Temps, F.; Wagner, H. Gg.; Wolf, M. *Ber. Bunsenges. Phys. Chem.* **1992**, *96*, 1043−1047.

(25) Dombrowsky, Ch.; Wagner, H. Gg. *Ber. Bunsenges. Phys. Chem.* **1992**, *96*, 1048−1056.
(26) Ashford, M. N. R.; Fullstone, M. A.; Hankock, G.; Ketley, G. W. *Chem. Phys.* **1981**, *55*, 245−257.
(27) Langford, A. O.; Petek, H.; Moore, C. B. *J. Chem. Phys.* **1983**, *78*, 6650−6659.
(28) Lee, P.-F.; Matsui, H.; Wang, N.-S. *J. Phys. Chem. A* **2012**, *116*, 1891−1896.
(29) Eskola, A. J.; Wojcik-Pastuszka, D.; Ratajczak, E.; Timonen, R. S. *Phys. Chem. Chem. Phys.* **2006**, *8*, 1416−1424.
(30) Welz, O.; Savee, J. D.; Osborn, D. L.; Vasu, S. S.; Percival, C. J.; Shallcross, D. E.; Taatjes, C. A. *Science* **2012**, *335*, 204−207.
(31) Alvarez, R. A.; Moore, C. B. *J. Phys. Chem.* **1994**, *98*, 174−183.
(32) Lu, K. W.; Matsui, H.; Huang, C.-L.; Raghunath, P.; Wang, N.-S.; Lin, M. C. *J. Phys. Chem. A* **2010**, *114*, 5493−5502.
(33) Wu, C.-W.; Matsui, H.; Wang, N.-S.; Lin, M. C. *J. Phys. Chem. A* **2011**, *115*, 8086−8092.
(34) Friedrichs, G.; Wagner, H. Gg. *Z. Phys. Chem.* **2001**, *215*, 1601−1623.
(35) Gannon, K. L.; Blitz, M. A.; Pilling, M. J.; Seakins, P. W.; Klippenstein, S. J.; Harding, L. B. *J. Phys. Chem. A* **2008**, *112*, 9575−9583.
(36) Srinivassan, N. K.; Su, M.-C.; Michael, J. V. *J. Phys. Chem. A* **2007**, *111*, 3951−3958.
(37) Chang., J.- G.; Chen, H. − T.; Xu, S.; Lin, M. C. *J. Phys. Chem. A* **2007**, *111*, 6789−6797.
(38) Hatakeyama, S.; Bandow, H.; Okuda, M.; Akimoto, H. *J. Phys. Chem.* **1981**, *85*, 2249−2257.
(39) Yamaguchi, K.; Ohta, K.; Yabushita, S.; Fueno, T. *J. Chem. Phys.* **1978**, *68*, 4323−4324.
(40) Kahn, S. D.; Hehre, W. J.; Pople, J. A. *J. Am. Chem. Soc.* **1987**, *109*, 1871−1873.
(41) Paulson, S. E.; Chung, M.; Hasson, A. *J. Phys. Chem. A* **1999**, *103*, 8125−8138.
(42) Oltzmann, M.; Kraka, E.; Gremer, D.; Gutbrod, R.; Andersson, S. *J. Phys. Chem. A* **1997**, *101*, 9421−9429.
(43) Anglada, J. M.; Bofill, J. M.; Olivella, S.; Sole, A. *J. Am. Chem. Soc.* **1996**, *118*, 4636−4647.
(44) Baulch, D. L.; Cobos, C. J.; Cox, R. A.; Frank, P.; Hayman, G.; Just, Th.; Kerr, J. A.; Murrells, T.; Pilling, M. J.; Troe, J.; Walker, R. W.; Warnatz, J. Evaluated kinetic data for combustion modeling, Supplement I. *J. Phys. Chem. Ref. Data* **1994**, *23*, 847−1034.
(45) Miyoshi, A.; Matsui, H.; Washida, N. *J. Chem. Phys.* **1994**, *100*, 3532−3539.